Geo-Marine Letters (2021) 41: 29
https://doi.org/10.1007/s00367-021-00700-z

ORIGINAL

Shelf architecture and recent sediment stratigraphy of the Chameis Bay area, southern Namibia

Heike Fourie[1,2] · Bjorn P. von der Heyden[1] · Kegan Strydom[3]

Received: 19 January 2021 / Accepted: 12 May 2021 / Published online: 29 June 2021

Abstract

Chameis Bay is located about 115 km north of the Orange River mouth and falls within the Sperrgebiet, an area which hosts the world's largest gem diamond deposit. Although significant quantities of diamonds have been recovered both on land and from offshore deposits in the Chameis Bay area, the marine geology of this important tract of coastline has not previously been described in the scientific literature. Here, we report the nearshore geomorphology and seismic stratigraphy offshore of Chameis Bay through analyses of bathymetrical and seismic datasets. These data have been complemented with lithogical data obtained from 70 reverse-circulation boreholes which helped to confirm and constrain the sedimentary stratigraphy of the study area. These datasets identified four major lithological units; viz. a Precambrian basement which predominates as the footwall in the nearshore regions of the study area, a Cretaceous clay unit that represents the offshore footwall lithology and two unconsolidated Cenozoic sedimentary units. The distribution of these unconsolidated sediments is strongly controlled by the ambient accommodation space which can be quantified by considering the architecture of the respective footwall units. Architectural features within the study site include two prominent wave-cut platforms, two coast-parallel sea cliffs, and a shelf-break formed at the contact between the Precambrian basement and the Cretaceous clay footwall. Accommodation space exists on the seaward of the two wave-cut platforms, which is cut into the Precambrian basement footwall and which lies below the fair-weather wave base, and at the break in slope at the contact between the two footwall units. The former accommodation space is most notable for gravel entrapment and preservation since gulley-controlled jointing and erosional depressions at lithological contacts represent 'fixed' trapsites from which coarse material is less likely to be remobilised. In contrast, the trapsites formed on the soft Cretaceous clay footwall are regarded as 'mobile' trapsites since they can be easily reconfigured by continuing erosional processes. As a result, the gravel bodies found above the Cretaceous clay are generally thin and poorly developed. The implications of these two different trapsites are briefly discussed in terms of diamond preservation potential, where anticipated diamond sources to the Chameis Bay near-shelf include the Orange River mouth as well as material that has been reworked from proximal sources. These results represent the first detailed description of the marine geology of the Chameis Subterrane thrust sheet and complement existing understanding of the Sperrgebiet's marine geology which largely derives from study sites on the Oranjemund Subterrane where linear beaches predominate.

Introduction

The southern African western margin hosts the world's largest placer diamond accumulation; a so-called diamond 'mega-placer' that spans the South African north-west coast, the lower reaches of the Orange River (a point source into the marine domain), and both offshore and onshore along the southern Namibian coastline (see De Wit et al. 2016 for a recent review). As the land-based diamond resources (e.g. river terraces and raised beaches) of this world-class deposit are increasingly being depleted, scientific attention and mining industry operations are increasingly focused on the offshore marine resources, which are typically more difficult

This article is part of the Topical Collection on *Coastal and marine geology in Southern Africa: alluvial to abyssal and everything in between*

✉ Bjorn P. von der Heyden
bvon@sun.ac.za

[1] Department of Earth Sciences, Stellenbosch University, Private Bag X1, Matieland, Stellenbosch 7602, South Africa

[2] Tect Geological Consulting, Unit 3, Metrohm House, 20 Gardner Williams Avenue, Cape Town 7130, South Africa

[3] Namdeb Diamond Corporation (Pty) Ltd, PO Box 253, Oranjemund, Namibia

to delineate and extract and have thus not yet been fully exhausted. As with any sedimentary system, these offshore marine resources are best understood by applying sound sedimentological first principles, viz. by considering both the autocyclic controls (e.g. sediment supply and hydrodynamic regime) and allocyclic controls (e.g. regional tectonism and eustatic sea-level changes) on the system (Beerbower 1964; Cecil 2003). Indeed, recent studies focused on the marine geology of the southern African mega-placer system have applied these first principles (Kirkpatrick and Green 2018; Kirkpatrick et al. 2019a,b; Runds et al. 2019)—an approach which has been greatly facilitated by technological advancements in geophysical techniques (e.g. seismic, electromagnetic and bathymetric data collection) and by collection of geochronological constraints on discrete sedimentological units (e.g. radiocarbon dating (Kirkpatrick et al. 2019a; Runds et al. 2019)).

An emerging theme that derives from this body of research is that in addition to the generally considered autocyclic and allocyclic controls, an important control on sediment and diamond distribution on the southern African west coast is imparted by the antecedent geology and associated shelf architecture/geomorphology (Kirkpatrick and Green 2018; Kirkpatrick et al. 2019b). For example, at a study area proximal to and immediately north of the Orange River mouth, Kirkpatrick and Green (2018) have illustrated how Proterozoic-aged structural geology controls the coastline orientation, distribution of local coastline knickpoints, and the slope and elevation of the near-shore geomorphology. At the same study site, Kirkpatrick et al. (2019b) have shown how diamond grade distributions are influenced by geomorphological features such as the gradient of the bedrock and the width of the local wave-cut platform. Further north, approximately 65 km from the Orange River mouth, Runds et al. (2019) have shown that preservation of a gravel barrier beach complex is largely attributed to the ambient shallow paleobathymetric slope coupled with a rapid rise in the relative sea level.

Whereas the aforementioned study sites are located relatively proximal to the Orange River mouth, which represents the modern outfall point for diamonds emanating from the Kaapvaal Craton, the marine geology of the more distal, yet still diamondiferous Chameis Bay area has not yet been fully described in available scientific literature. Chameis Bay is located approximately 115 km north-west of the Orange River mouth and represents an important regional change in orientation of the southern Namibian coastline, from NW (~ 134°) trending to NNW (~ 151°) trending (Fig. 1). Several published observations highlight that the selected study area is deserved of special scientific attention. These include (1) the dominant beach morphology changes abruptly from linear beaches in the south to pocket beaches in the north;

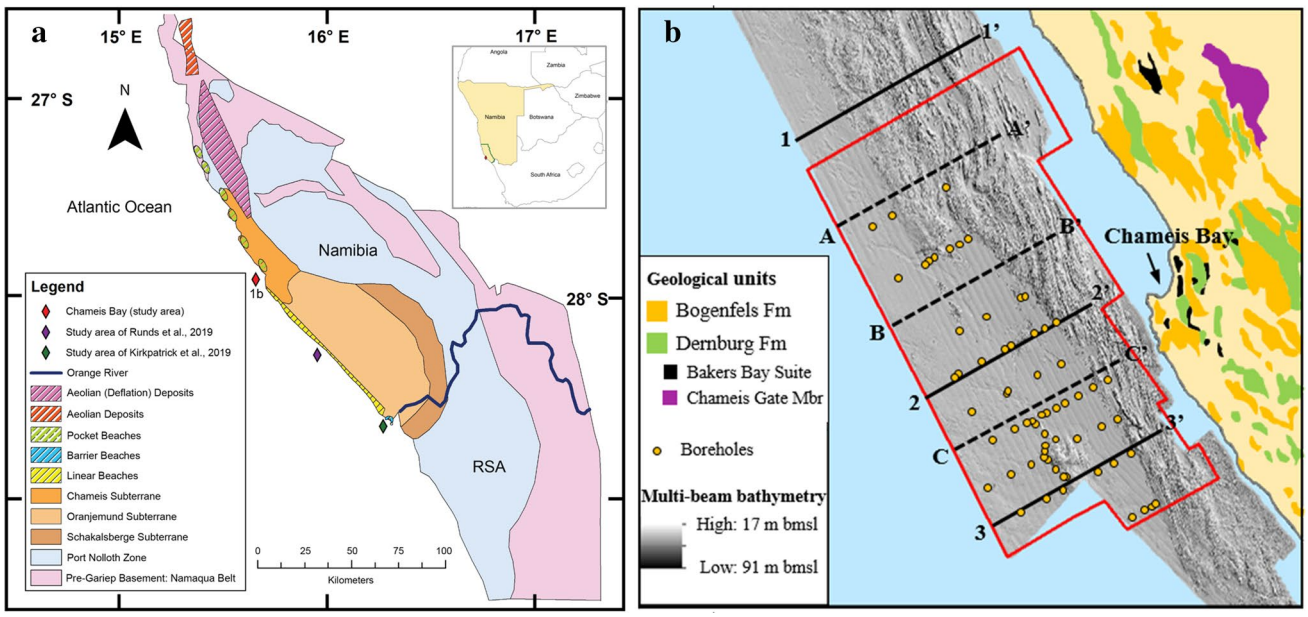

Fig. 1 **a** Regional geological overview of the southern African diamond mega-placer coastline adjacent to the Gariep Belt in southern Namibia and northwestern South Africa. The locations of the Purple Target Area (Runds et al. 2019) and Oranjemund study area (Kirkpatrick et al. 2019a,b) are indicated since they represent previous seismic studies conducted on the same sedimentary mega-placer system. Inset map shows the position of the Sperrgebiet (green outline) and Namibia relative to the rest of southern Africa. **b** Multi-beam bathymetry map of the study area showing the adjacent on-land local geology (redrawn after Frimmel 2018). Solid lines 1–1′, 2–2′ and 3–3′ indicate the positions of the seismic profiles presented in Fig. 3, whereas dashed lines A–A′, B–B′ and C–C′ are the additional sections used in the integration procedure

(2) the dominant gulley morphology also shows a marked change from a swash-parallel and strike-parallel gulley in the south to joint-controlled gulley orientations (60–70° and 120–140°) in the Chameis Bay area (Jacob et al. 2006); (3) Chameis Bay area has been experienced significantly more down-warping relative to the southern regions of the coastline (Jacob 2016); and (4) the Chameis Bay study site is situated on the Chameis Subterrane of the Marmora Terrane, as opposed to more southerly study sites which are located on the Oranjemund Subterrane (Frimmel 2018 and references therein). Using seismic and bathymetric data, the present contribution seeks to describe the nearshore geomorphology and seismic stratigraphy of the marine geology offshore of Chameis Bay. This contribution extends the existing understanding of the marine geology of southern Namibia's diamondiferous coastline (Kirkpatrick and Green 2018; Kirkpatrick et al. 2019a,b; Runds et al. 2019) and will augment the body of work conducted on the adjacent onshore diamond areas of the Sperrgebiet (e.g. Kalbskopf 1987; Jacob et al. 2006).

Regional setting

Regional and local geology

Very little published information exists for the marine geology offshore of Chameis Bay. A similar situation exists for the corresponding onshore geology, largely on account of limited outcrop exposure and because of relatively limited historical access to the Sperrgebiet diamond tenements. Notwithstanding the above and notwithstanding the inherent limitations associated with extrapolating onshore geology to offshore geology, the study area is expected to be underlain by basement rocks formed during the Pan-African Gariep orogenic cycle. This orogenic belt (along with the more southern Saldania Belt in South Africa) records an extended Neoproterozoic-to-Cambrian Wilson Cycle associated with opening and subsequent closure of the Adamastor Ocean, an analogue of the modern-day South Atlantic Ocean. The Gariep Supergroup is broadly subdivided into the para-autochthonous Port Nolloth Zone which comprises predominantly continental lithostratigraphy, and the allochthonous Marmora Terrane which comprises predominantly oceanic lithostratigraphy (Frimmel 2018 and references therein). The Chameis Bay study area is located in the Chameis Subterrane—the uppermost thrust sheet of the Marmora Terrane which tectonically overlies the Oranjemund and Schakalsberg thrust sheets (Fig. 1a). The Chameis Subterrane comprises metabasic rocks of the basal Dernberg formation, mafic to ultra-mafic rocks of the Bakers Bay Suite, glaciogenic diamictites of the Chameis Gate Member and metasedimentary rocks of the Bogenfels Formation which represent the youngest rocks in the area (Fig. 1b; Frimmel 2018). The tectonic contact between the Chameis Subterrane and the underlying siliclastic-dominated Oranjemund Subterrane has an inferred location several kilometres to the SE of the study area (Fig. 1a). The location of this contact broadly correlates with a change in the coastline architecture (Fig. 1a), where linear beaches dominate in the south (Oranjemund Subterrane), whereas pocket beaches become more prevalent to the north (Chameis Subterrane).

Chameis Bay study site

The Chameis Bay study area is defined by a ~ 19.5-km-long coast-parallel strip located between 0.9 and 3 km offshore of the present coastline (Fig. 1b). It is situated on the inner shelf (water depths range between 17 and 91 m bmsl) at a location approximately 115 km north of the Orange River mouth. From an economic standpoint, the study site is deemed prospective for alluvial diamonds since the only prior marine exploitation of the area occurred during the 1960s at depths less than 30 m bmsl and more than 100 m bmsl (Williams 1996; Richardson 2007). The corresponding land-based exploitation of alluvial diamonds in the Chameis Bay region focused on shore platforms where alluvial diamonds were predominantly won from pocket beaches located 2 m above the present mean sea level (Apollus 1995).

The southern African west coastline is characterised by an exceptionally high wave energy regime in which the dominant swell direction is from the south west (e.g.Compton et al. 2002; Bluck et al. 2007). This facilitates sculpting of the embayed coastline from Chameis Bay northwards by differential erosion of the variably resistant rock units (Davies 1964). It also facilitates efficient sediment transport dynamics within the broader mega-placer system, notably resulting in northward redistribution of alluvial diamonds and coarse sediments from the Orange River mouth by longshore drift (Robert et al. 2005; Jacob et al. 2006; Spaggiari et al. 2006; Bluck et al., 2007; de Wit et al., 2016). This northward redistribution of the Orange River coarse sediment load towards the Chameis Bay study area is enhanced by the equatorward flow of the Benguela current as well as by the action of southeasterly trade winds (Robert et al. 2005). Additional sediment inputs into Chameis Bay area derive from a local, non-perennial river (relatively small drainage extent) which transports proximal material into the marine setting.

Methods

Geophysical data

The study area was covered by RESON 8101 multi-beam bathymetry survey, illustrating topographical variations

and sedimentary features of the seafloor. The multi-beam bathymetry has an approximate binned horizontal resolution of 5 × 5 m (X and Y) and an approximate vertical resolution of 1 m (Z). The resolution of the bathymetry is of such quality that it can be used to differentiate between the Precambrian bedrock and sediment cover, along with identifying various topographical features such as scours, bedforms and bedrock structures such as potholes and gullies (Fig. b1; Green 2009).

The study area comprises a total of 52 seismic profiles (~ 424 km) of single-channel Sparker data collected between water depths of 17 and 91 m bmsl. Sparker is a medium penetration and medium resolution signal, with a vertical resolution of 1–1.5 m. The seismic survey lines are orientated in an approximately northeast–southwest direction and intersect the continental margin at a perpendicular angle. The Sparker lines are separated by a 400-m spacing, except in the central region, where the line spacing is reduced to approximately 100 m. Processing and interpretation of the seismic lines were undertaken in GeoSuite AllWorks software, where gain was applied to all the sections to enhance the signal for interpretation purposes. Thereafter, various stratigraphic horizons were interpreted through a combination of automated and manual editing, by digitising high amplitude reflectors and by digitising variations in seismic facies. Each unit encountered within the study region displayed a unique geophysical characteristic. This was determined from the seismic analysis and similar geological domains were identified based on these geophysical characteristics. The various seismic horizons were converted from two-way time (TWT) to depth (in metres) by using constant velocities of 1500 m/s for seawater and 1600 m/s for sediments. For validation purposes, boreholes in the study area were correlated to the interpreted horizons of corresponding seismic sections (Fig. 2).

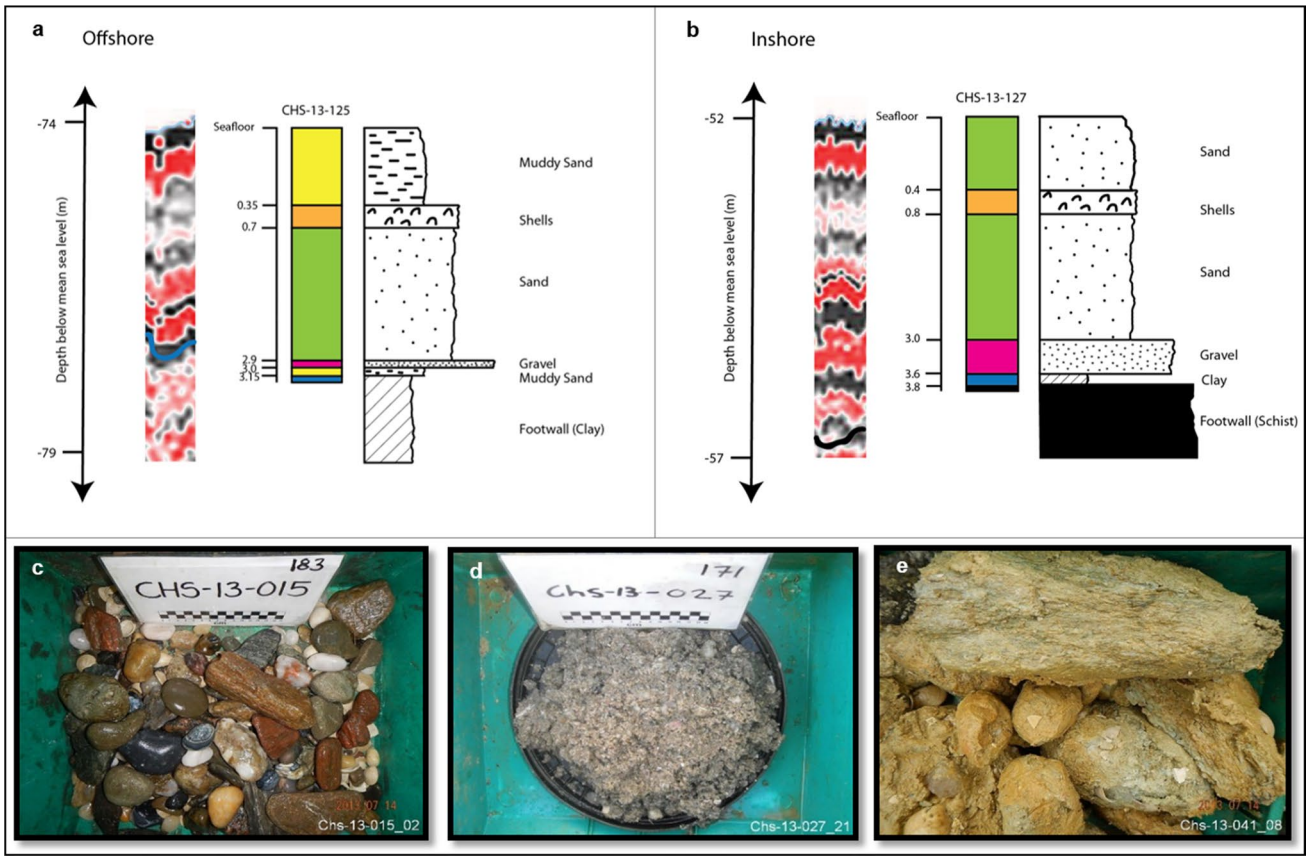

Fig. 2 **a, b** Representative stratigraphic sections comparing the seismic stratigraphy with the closest borehole logs obtained from the reverse circulation drilling campaign. The seismic profiles were unable to discern subtle stratigraphic variations at the sub-metre scale, whereas the borehole data provides richer insights into the stratigraphy and, importantly, gravel distributions. **c, d** Representative examples of the sediment material recovered from the reverse circulation drilling campaign. **c** Coarse gravel fraction (> 19 mm diameter) comprising rounded to sub-rounded predominantly exotic gravels. **d** Fine sand fraction (< 1.4 mm diameter). **e** Precambrian bedrock represented by Gariep Belt schists (Bogenfels Fm?) that have been partially altered to saprolite

Geological data

Lithological data was acquired from the borehole logs recorded by various Namdeb field geologists for 70 boreholes (Pether 2013a, b) interspersed throughout the study area (Fig. 1b). The boreholes were drilled using a 5-m^2 reverse circulation (RC) drilling apparatus which is capable of drilling to a depth of 12 m, but a maximum drill depth of 7.8 m was achieved in the study area. The boreholes were drilled as part of an exploration drilling campaign and did not follow a gridded drilling pattern, instead being selected based on the analysis of the seismic interpretations and the multi-beam bathymetry. Drilling was limited to areas within the study site where the water depth exceeded 30 m due to restrictions associated with the sampling vessel. Three of the boreholes were aborted due to technical limitations and the majority of the boreholes were terminated when the drill intersected the footwall lithologies (Cretaceous-aged clay, or Precambrian schists or mafic/volcanic bedrock). The samples collected during the drilling campaign were separated according to grain size; coarse-grained material (diameter > 19 mm) and fine-grained material (maximum diameter < 1.4 mm). When a change in the lithology was noted, the samples were collected in separate sample bins (Fig. 2).

Quantifying accommodation space

Six seismic profiles, distributed evenly across the study area, were selected for a more detailed evaluation of the available sediment accommodation space (Fig. 1b). The seismic depth data was converted from two-travel time to depth intervals (see Sect. 3.1), whereas the projected geographic (WGS84–33S projection) X–Y data were converted into distance values using the distance formula and the 90 m bmsl basement-rock elevation contour as an origin. These processed data were then imported into the spectral processing software WinXAS (Ressler, 1998) for integration (Fig. 3). Each of the processed seismic sections was integrated over the linear distance between 90 m bmsl basement-rock elevation contour and the 35 m bmsl basement-rock elevation contour (due to the constraints of the available data). The integration procedure was conducted for the present sea-level stand, as well as for – 15, – 30, – 45, – 60 and – 75 m bmsl. The measure is at best a proxy for the accommodation space at various sea-level stands since it does not take into account any geomorphological sculpting of the basement rock architecture as a function of changing sea level with its associated erosional and/or depositional processes. An additional integration procedure was conducted using the seismic-interpreted thickness data for the sediment layers overlying the basement lithologies. This was conducted using the same six seismic lines and the same linear interval described previously (i.e. segment between the – 90 m basement contour and the – 35 m basement contour).

Results

Bathymetry

The sea-floor bathymetry within the study area ranges in depth between 17 and 91 m bmsl, with an average depth across the entire area of around 57 m bmsl. The shallower areas generally coincide with the rugged textures observable on the bathymetric map (Fig. 1b) which are more prevalent in the northern half of the study area. These rugged textures represent the exposed areas of Precambrian bedrock, which typically show an undulating pattern (Miller et al. 2000) and which have an apparent strike orientated in a NNW direction (Fig. 1b). In the deeper waters and trending perpendicularly offshore from Precambrian bedrock, the bathymetric signal reflects a smooth even-toned texture representing a veneer of more recent, unconsolidated sediment. The distribution

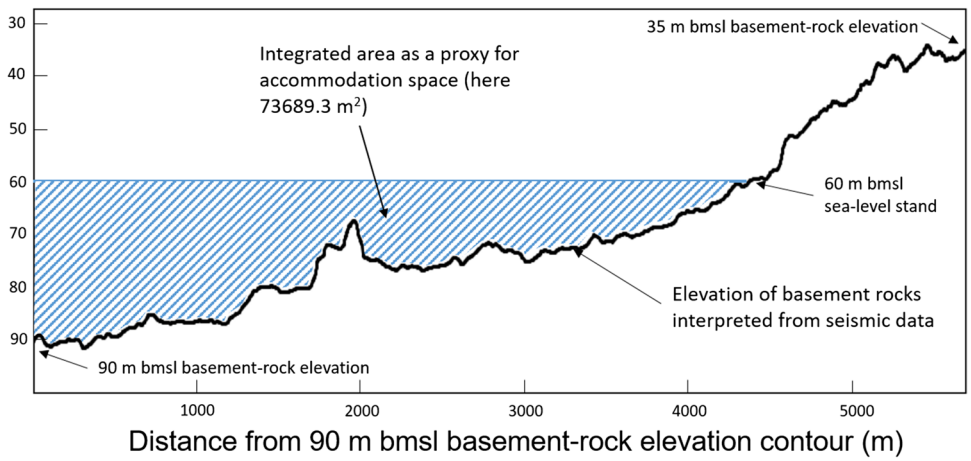

Fig. 3 Schematic illustrating the area that was integrated as a proxy for the accommodation space for sediment accumulation. Interpreted seismic section is line B–B′ and the integration occurred between 35 and 90 m bmsl footwall elevation depth contours and a modelled sea-level stand that is 60 m bmsl

of this material is most extensive in the south of the study area where it trends in a NW direction parallel to the modern coastline. Towards the north of the study area, the breadth of the sediment covered area pinches out against a tongue of shallower Precambrian bedrock.

Geophysical and geological stratigraphic units

The interpretation of the seismic profiles (Fig. 4) from the study area revealed four major seismic units (units 1–4) and four seismic horizons (horizons 1–4). Interpretation of the borehole logs in conjunction with the seismic data was used for the identification of the various stratigraphic units. Table 1 summarises these results and compares the identified units to those previously described by Runds et al. (2019) and Kirkpatrick et al. (2019a). The reasons for these comparisons are that (1) Chameis Bay, Purple Target Area (PTA) and the Oranjemund study sites all fall within the greater Orange River–Sperrgebiet mega-placer sedimentary system; and (2) detailed geochronological data exists for the PTA and Oranjemund study sites (Runds et al. 2019; Kirkpatrick et al. 2019a), thus accurate correlation will promote disentanglement of the Chameis Bay recent sedimentary history. The identified seismic stratigraphic units are described in geochronological order (viz. from oldest to youngest). Descriptions of each seismic stratigraphic unit are followed by corresponding lithofacies' descriptions derived from observations made during the reverse circulation drilling programme.

Unit 1: Precambrian bedrock

Seismic observations Unit 1 is present throughout the study area and forms the inshore portion of the acoustic basement. It is characterised by high-amplitude chaotic reflectors with no coherent or continuous internal reflector geometry (Fig. 4). It has a rugged external morphology and becomes acoustically transparent with depth. Unit 1 is capped by the high-amplitude horizon 1 that forms pinnacles, ridges and gullies across the inshore portion of unit 1 and dips steeply beneath unit 2 towards the offshore edge of the study area. It is characterised by a break-in-slope between 77 and 80 m bmsl in the south of the study area and > 85 m bmsl depth towards the north.

Lithological observations Several boreholes intersected the crystalline basement lithology which was identified predominantly as a schistose unit (Fig. 2b, e). This schist ranged in colour between dark grey-brown to yellow–brown and, from its mineralogy, was identified as a quartz–mica schist. In some instances, the intersected bedrock was highly weathered to a brownish-grey saprolite which was largely devoid of internal structures. The extent of weathering negated a definitive identification of its precursor lithology, which may have been the quartz–mica schist or some other lithology found in the Chameis Subterrane (Fig. 1b).

Unit 2: Cretaceous clay

Seismic observations Unit 2 represents the other lowermost lying unit, located towards the offshore of unit 1. Unit 2 can be seen to contain a large amount of small depressions throughout the unit, with the majority occurring on the landward section closer to the contact with the unit 1 footwall. Unit 2 displays chaotic reflections of varying amplitude, with occasional coherent reflectors visible to be dipping at a shallow angle seaward. Unit 2 is capped by a comparatively high amplitude relatively rugged surface, named horizon 2.

Lithological observations Numerous boreholes intersected unit 2 within the study region and this footwall was identified as a clay unit (Fig. 2a). The colour for this unit varied from a dark green-olive, to grey to a red-orangey brown. The texture of the clay was described as being soft and firm to hard, and in one instance having a more silty-muddy composition. Sand and pebble inclusions occurred sporadically within this unit, where pebbles of schist from the adjacent unit 1 were also encountered. Internal features, such as flame structures and laminations, were identified within this clay unit. Unit 2 was identified previously as being composed of sedimentary rocks of Albian to Cenomanian (Early Cretaceous) age by other authors (e.g. Dingle et al. 1983) and Unit 2 was therefore identified as a Cretaceous clay. Based on borehole data and previous studies, the Cretaceous succession was deduced to have been deposited by a fluvial system.

Unit 3: poorly developed gravel bodies

Seismic observations Unit 3 unconformably overlies units 1 and 2 and is generally separated by a relatively high-amplitude surface (i.e. either horizon 1 or horizon 2). Unit 3 occurs as small localised heaps which commonly show a very subtle seaward dip (Fig. 3). Most observations of this unit indicate that it is found preferentially at elevations of between − 50 and − 70 m bmsl in the depressions and scours formed at the surface of unit 1. The encountered unit was not continuous and could not be traced between adjacent seismic lines. Due to the low resolution of the Sparker data and relatively thin nature of unit 3, confidently identifying this unit was not always achievable. Unit 3 is capped by a high-amplitude surface named horizon 3 (Table 1).

Lithological observations Borehole data identified unit 3 as a mixture of angular to sub-angular clasts and rounded to sub-rounded clasts. The size distribution ranged from cobbles to pebbles and the thickest unit intersected was 2.5 m

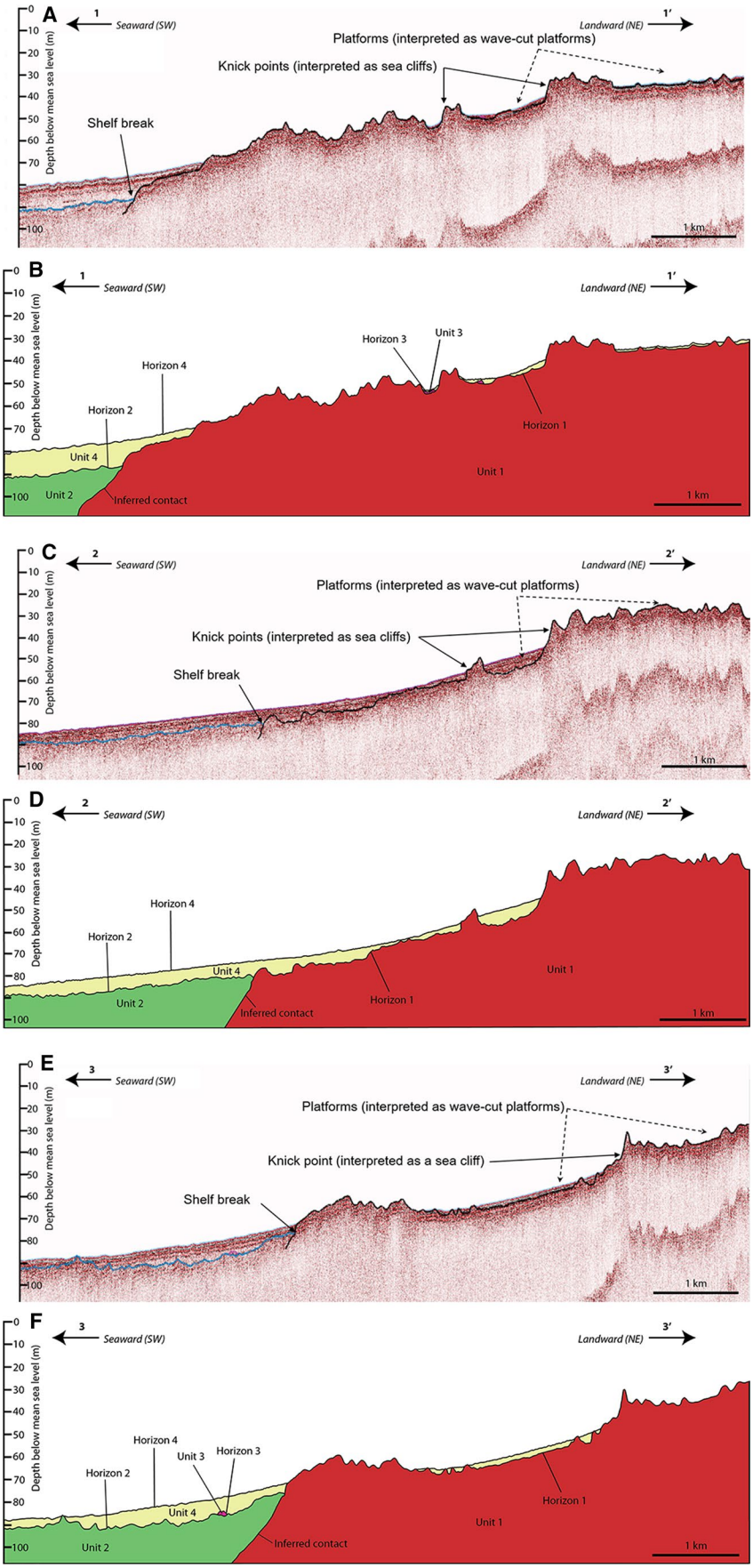

Fig. 4 Representative Sparker seismic transects collected across the inner shelf region of the study area, with 20 × vertical exaggeration (see Fig. 1b for transect locations). Each of the units and their corresponding horizons are described in Sect. 4.2 in the main text. **a, b** Seismic section and corresponding annotated interpretation schematic for the northernmost transect located ~ 10 km north of Chameis Bay. **c, d** Seismic section and corresponding annotated interpretation schematic for a representative transect located directly offshore of Chameis Bay. **e, f** Seismic section and corresponding annotated interpretation schematic for a representative southerly transect located ~ 6 km south of Chameis Bay

Table 1 An overview of the seismic stratigraphy of the Chameis Bay study area, with correlations drawn to units previously described by Runds et al. (2019) in the Purple Target Area (PTA) located ~ 50 km south, and to units described by Kirkpatrick et al. (2019a) at the Orange River mouth located ~ 115 km south

Unit	Horizon	Internal reflection geometry	Description	Thickness (m)	Primary lithology	Correlation to PTA	Estimated period/ epoch for units at PTA	Correlation to Orange River	Estimated period/ epoch for units at Orange River
	Horizon 4		High amplitude and undulating, sometimes rippled surface, capping unit 4						
Unit 4		Low amplitude, continuous, relatively horizontal reflective signatures	Unconformably overlies units 1, 2 and 3	≤ 10	Muddy sand, sand, shelly sand	Unit 4 can be correlated to unit D, composed of acoustically homogenous, low-amplitude, semi continuous, subparallel reflectors, lithologically identified as gravel, sand and muddy sand	Early to Late Holocene	Unit 4 can be correlated to unit 7 defined by seaward dipping parallel reflectors displaying a variety of continuity, as well as amplitude comprised of muds and sands	Holocene Radiocarbon dates of 8 to 0.89 ka and 5 to 0.83 ka from *Macoma* valve and *Nassarius vinctus* snail, respectively
	Horizon 3		High-amplitude surface, capping unit 3						
Unit 3		Moderate to low amplitude reflective signatures, with some coherent reflectors displaying very subtle seaward dip	Unconformably overlies unit 1 and unit 2 and occurs as small, discontinuous heaps concentrated in depressions	≤ 2.5	Angular to rounded clastic, polymictic material			Unit 3 of Chameis Bay can be correlated to unit 4, composed of a single, high-amplitude reflector, with an average thickness of ~ 2 m and occurs throughout the study region, but can be seen to be concentrated within gullies of the bedrock units. Interpreted to be a gravel lag deposit	Holocene Radiocarbon dating of *Choromytilus* sp. and *Tellina* sp., obtained from the middle of unit 4 at lower shoreface palaeodepths (6–12 m), produced age range of 10.6–10.2 ka
	Horizon 2		Comparatively high-amplitude, relatively rugged surface and caps unit 2						

Table 1 (continued)

Unit	Horizon	Internal reflection geometry	Description	Thickness (m)	Primary lithology	Correlation to PTA	Estimated period/ epoch for units at PTA	Correlation to Orange River	Estimated period/ epoch for units at Orange River
Unit 2		Chaotic reflections of varying amplitude, with occasional coherent reflectors visible to be dipping seaward at a shallow angle	Lowermost lying unit, located towards the offshore. Relatively rugged texture		Clay	Units 1 and 2 collectively can be correlated to unit A of low-amplitude, gently seaward dipping parallel reflectors determined to be Neoproterozoic and mid-Cretaceous acoustic basement	Mid-Cretaceous	Unit 2 of Chameis Bay can be correlated to the medium to high-amplitude, often hummocky and chaotic reflectors of unit 2 of the Orange River setting that defines the offshore dipping basement	Albian to Cenomanian (Early Cretaceous)
	Horizon 1		Caps unit 1. Forms pinnacles, ridges and gullies across the inshore portion						
Unit 1		Streaky to acoustically transparent, chaotic, mottled reflections, with no coherent or continuous internal reflectors	One of the lowermost lying units on the inshore portion. Dips towards the offshore. Displays a rugged external morphology		Phyllites, schists and saprolites		Neoproterozoic	Unit 1 of Chameis Bay can be correlated to unit 1 of the Orange River setting with high-amplitude, highly chaotic and rugged texture defining this basement unit	Neoproterozoic

and the thinnest 0.04 m (Fig. 5a). Unit 3 was composed of a variety of gravel compositions, representing a mixture of proximal and distal sources (Fig. 2a–c). The major constituents of this unit were quartz, quartzite, volcanoclastic material, sandstones, conglomerates and dolomite. The exotics, indicative of a distal source, were noted as agates, jaspers, chalcedony, banded iron formations (BIFs), epidosites and makwassie quartz porphyry (Pether 2013a, b).

The drill-hole pattern did not allow for a comprehensive overview of the gravel distributions within the study area. Despite this paucity in available drill-hole data, the gravels appear to be sporadically developed within the study area, with an apparent preferential development in the offshore lee of the basement highs (where the total unit 3 + 4 stratigraphic thickness is generally quite thin (Fig. 5a)). One of the boreholes intersected three individual layers of gravel interbedded with sand, five of the boreholes intersected two layers of gravel interbedded with sand, whereas the remainder of the boreholes intersected either one layer of gravel or no gravel at all (Fig. 5a).

Unit 4: Cenozoic sediments

Seismic observations Unit 4 unconformably overlies units 1, 2 and 3 and comprised low-amplitude reflective signatures that separate this unit from the underlying units (Fig. 3). This unit displays parallel, horizontally continuous properties. Unit 4 is capped by horizon 4, a high-amplitude, and undulating, sometimes rippled surface representing the seafloor.

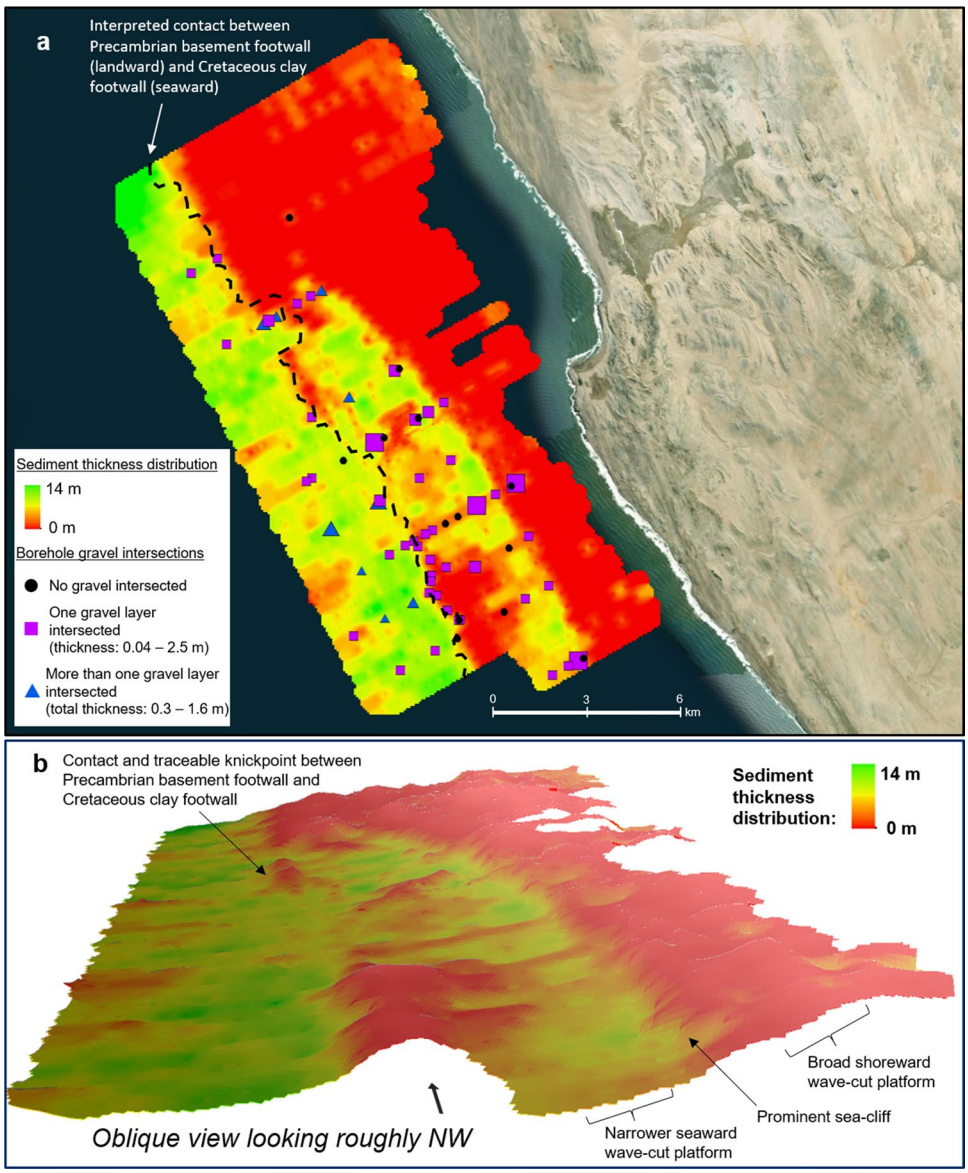

Fig. 5 **a** Interpreted sediment thickness distribution (seismic units 3 + 4) for the study area. Symbology overlay represents the number and culminated thickness of the gravel layers intersected during the Reverse Circulation drilling campaign. Squares represent a single gravel layer whereas triangles represent boreholes where more than one gravel layer was intersected. Both symbol sets are graduated (by size) into four categories: < 0.4 m, 0.4–0.6 m, 0.8 m and > 0.8 m thick. **b** The same seismic sediment (unit 3 + 4) thickness distribution data draped on the footwall elevation data derived from seismic interpretation. The elevation data has a vertical exaggeration of 20 times

Lithological units The borehole intersections revealed that unit 4 comprises unconsolidated sediments ranging from muds to fine sands to relatively coarse gravels (Fig. 2a–d). Sedimentary layering and the presence of discrete stratigraphic sub-units (within unit 4) were observed in the sediment recovered from the boreholes. Due to the low resolution of the Sparker seismic data, these units could not be distinguished individually in the seismic sections. The overall thickness of the unit 4 sedimentary package extends up to 10 m. The sub-units that collectively make up unit 4 range in thickness, with the thinnest sub-unit having a thickness of 0.005 m and a maximum of 6 m (average thickness 0.64 m).

On the basis of the borehole sampling, unit 4 can be subdivided based into two categories that are spatially linked to the basement lithologies (units 1 and 2). Where located over unit 1 (Precambrian basement), unit 4 comprises a basal gravel layer overlain by sand (Fig. 2b). In contrast, the offshore regions in which unit 2 (Cretaceous clay) is the footwall, the recent sedimentary package generally comprises a basal sand layer, overlain by sand, then gravel, then another sub-unit of sand, and finally the topmost sub-unit consisting of a shelly to muddy sand (Fig. 2a). In the individual subunits identified, upward-fining grainsize distributions were commonly observed.

Footwall architecture

Three coast-perpendicular Sparker seismic Sects. (1–1′; 2–2′; 3–3′ (Figs. 1 and 4)) were selected for detailed presentation here, since they are representative of the geographic changes in the shelf architecture and stratigraphy along a N–S transect of the study area.

Northern transect

Figure 4a and b depicts a seismic section that is representative of the northern part of the study area. This northern part clearly shows an extensive inner-shelf region in which the resistant Precambrian basement lithology dominates the exposed geology. The region is characterised by a relatively gentle gradient and a series of platforms separated by prominent knickpoints. A broad (> 1 km breadth) platform is found at approximately 35 m bmsl, and a second ~ 900 m broad platform dips gently between 42 and 50 m bmsl. These platforms are veneered by unconsolidated sediments (units 3 and 4), which have increasing stratigraphic thickness on the deeper-water platform. The two platforms are separated by a ~ 10-m-high sea knickpoint at 32–42 m bmsl. A second ~ 7-m-high knickpoint is found at a depth ranging between 45 and 52 m bmsl. At water depths between 45 and 85 m bmsl, the Precambrian bedrock persists as the footwall unit. It displays a rugged, eroded topography and from seismic interpretations (Fig. 4), very little recent (Cenozoic) sediment appears to have accumulated in the sporadically developed troughs. A regional knick-point exists at the contact between the Precambrian basement rocks and the Cretaceous clays (~ 87 m bmsl). The Cretaceous clay is a relatively soft footwall unit and is characterised by a series of small amplitude depressions along its surface (horizon 2). Most of the recent sediment accumulation is constrained to this deeper water setting (i.e., 70–92 m bmsl) where thick packages of unit 4 have built up (up to ~ 10 m thick).

Central transect

The shelf architecture of the central region of the study site is depicted in Fig. 4c and d. Again, the Precambrian basement lithology dominates in the landward extremity of the transect where it results in a shallow platform (~ 28 m bmsl) which is devoid of significant sediment accumulation and is characterised by a shallowly dipping gradient. The prominent knickpoint described for the northern transect can be traced into the central part of the study area where it increases in height (~ 21 m), but occupies a similar depth below the current sea level (i.e. 31–52 m bmsl). A second narrower 750 m platform is found at depths between 50 and 57 m bmsl, and is overlain by approximately 5 m of Cenozoic sediments (unit 4). A second ~ 10-m-high knickpoint, again correlatable to the one described in the north, is found at water depths between 50 and 60 m bmsl. The Precambrian footwall then continues to dip moderately until the contact with Cretaceous clays (80 m bmsl), except where this trend is interrupted by a smaller ~ 3 m knickpoint at 69–72 m bmsl. A 5- to 7-m-thick sediment package covers the entirety of the offshore section of transect; from the base of the 10-m-high knickpoint to the 90 m footwall elevation contour (i.e. the end of the seismic section).

Southern transect

The southernmost transect presented herein (Fig. 4e, f) displays similar geomorphological features to the transects described to the north, although with a notable absence of the second deeper-water knickpoint. Again, the coast-proximal platform occupies depths < 38 m bmsl and is devoid of any notable sediment accumulation. The prominent and regionally traceable knickpoint is found at depths between 30 and 43 m bmsl, the base of which grades into a poorly developed (< 200 m broad) second platform which terminates at a ~ 4-m-high second knickpoint. The shelf then grades gently seaward for approximately 2 km and is veneered by ~ 2 m of Cenozoic sediments which pinch out against a resistant exposure of Precambrian bedrock which creates a section of high relative relief at ~ 60–73 m bmsl. The break in shelf, typified by the contact between the Precambrian bedrock

and the Cretaceous clay, is found at 78 m bmsl. The major recent sediment accumulation is found exclusively above this clay footwall, where sediment package (unit 3 + unit 4) thickness ranges between 5 and 10 m thick (Figs. 4e, f and 5). This sediment package includes sporadically developed gravel bodies which occupy a basal positioning on the undulating clay footwall.

Stratigraphic thickness distributions

Figure 5a provides a plan view of the recent sediment (unit 3 + unit 4) thickness distribution within the study area, whereas Fig. 5b shows the same data from an oblique viewpoint and overlain on the bedrock topography data interpreted from the seismic sections. The sediment thickness distribution throughout the study area ranges between 0 and 13.8 m thick, with an overall average of 3.0 m. The coast-proximal platform is largely devoid of any sediment accumulation except in sporadically developed erosional depressions and in the north where the platform is located deeper than 30 m bmsl and has a thin veneer of recent sediments. A distinctive coast-parallel band of sediment occupies the platform immediately below the dominant knickpoint feature. Upon this platform, the sediment thickness averages between 3 and 5 m thick in the south, is thickest in the central region (up to 7–10 m thick) and tapers out in the north (where the platform becomes narrower and shallower). A second prominent band of sediment is found in the offshore region of the study area and corresponds to distribution of the Cretaceous clay footwall lithology (unit 2). Here, the sediment package commonly ranges between 7 and 10 m thick, and is also where the maximum sediment thickness (~ 14 m) was measured.

Accommodation space

Accommodation space is defined as the space available for sediments to accumulate between the sea floor and a base level (Spaggiari 2011). In an attempt to quantify the accommodation space available in the Chameis Bay study area, we utilised an integration function (Fig. 3) to measure the available area between the footwall (Precambrian basement (unit 1) or Cretaceous clay (unit 2)) and a series of hypothetical sea-level positions (− 15 m, − 30 m, − 45 m, − 60 m and − 75 m). This theoretical treatment considered six seismic lines: the three described in Sect. 4.3 above (1–1′, 2–2′ and 3–3′) and three additional lines found at intermediate positions (Fig. 1b; A–A′, B–B′ and C–C′). The depth range that was considered was limited by the available data, and thus the measure of accommodation space was constrained to the region within the study area in which the footwall elevation was between 35 and 90 m bmsl.

Figure 6a shows the results of this integration exercise and highlights that the accommodation space decreases from the south (or southeast) to north (or northwest) irrespective of the sea-level stand at which the accommodation space is modelled. At the current sea level and among the six transects evaluated, the linear accommodation space between footwall depths of 35 and 90 m bmsl ranges between 390,000 and 510,000 m^2 (Fig. 6a). A notable step in this otherwise relatively linear S–N trend is located somewhere in the central part of the study area (i.e. between transect B–B′ and transect 2–2′). This step is most notable for the 0, − 15 and − 30 m sea-level stands and reflects the fact that the northern region is characterised by a relatively extensive and shallow near-shelf region. Figure 6b considers only the current sea-level stand and compares the integrated area for available accommodation space versus the integrated area of actual sediment accumulated. Both integrals were then normalised against the linear distance between the 35 m bmsl footwall contour and the 90 m bmsl footwall contour, to provide a final value in metres. A significant and positive correlation ($r^2 = 0.73$) exists between these two measures,

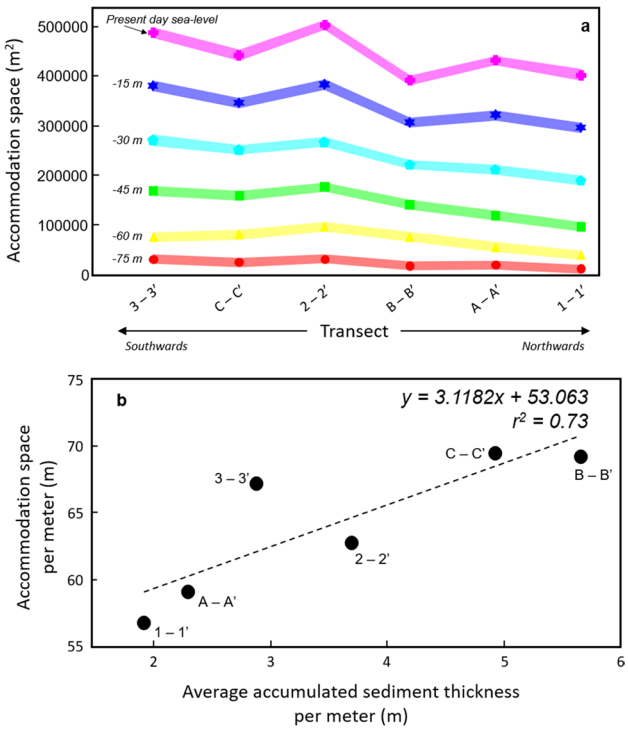

Fig. 6 **a** Results of the integration procedure for the six seismic transects considered in this study (Fig. 1b) modelled at six different hypothetical sea-level stands. A marked change in total accommodation space is clearly illustrated by the step change occurring between seismic lines 2–2′ and B–B′. **b** A linear regression plot between the total accommodation space and the total accumulated Cenozoic sediment thickness, where both parameters have been normalised to the length of each respective seismic transect (i.e. linear distance between the 35 and 90 m bmsl footwall elevation contours)

highlighting that a relationship exists between the available accommodation (within the constrained depth contours) and the quantity of sediment that has ultimately accumulated.

Discussion

An overview of the marine geology of Chameis Bay

The primary objective of the present contribution is to provide a descriptive overview of the shelf architecture, geomorphology and stratigraphy of the inner-shelf region near Chameis Bay. Such a comprehensive description does not yet exist in the available scientific literature, and should greatly augment the existing understanding of the marine geology of this important and diamondiferous coastline (Rau 2003; Stevenson and McMillan 2004; Bluck et al. 2007; Oelofsen 2008; Kirkpatrick and Green 2018; Kirkpatrick et al. 2019a,b; Runds et al. 2019).

In the Chameis Bay area, there are several notable features that are traceable throughout the E–W latitudinal sections of the study site (Figs. 4 and 5). These include (1) two broad platforms which we interpret as being wave-cut platforms formed during periods of sea-level slowstands or stillstands, (2) two prominent knickpoints which we interpret as being sea cliffs and (3) a shelf break marked by the contact between the Precambrian basement footwall (unit 1) and the Cretaceous clay footwall (unit 2). The shallower, landward of the two wave-cut platforms occurs at depths of around 35 m bmsl in the north and generally at shallower depths further south (e.g. ~ 28 m bmsl in the central transect (Fig. 4c, d)). This platform possibly correlates to the 28 to 30 m bmsl platform identified by de Decker (1986), the 30 m bmsl platform identified by Rau (2003), and the 27 m bmsl terrace identified by Oelofsen (2008). Notably, the deeper northern transect is veneered by a thin layer of recent sediment (Fig. 4a, b), whereas the shallower transects to the south are devoid of this covering (Fig. 4c–f). We attribute this to the scouring by wave action acting on the shallower platforms. This suggests that the wave base in the study area is around 35 m bmsl, a depth which is comparable to the fair-weather wave base (40 m bmsl) suggested previously for the southern Namibian coastline (Bluck et al. 2007; Kirkpatrick et al. 2019b). Progressing seaward, the shallow wave-cut platform is sharply terminated by a prominent sea cliff that ranges in height between 10 and > 20 m (Fig. 4a). This sea cliff will have formed by erosive wave-action operating at a paleo-shoreline during an earlier sea-level stillstand, which we estimate to have existed at ~ 42 m bmsl. This sea-level stand is similar to the − 40 m shoreline occupation described on southern Africa's east coast which has previously been linked to a regional − 46 to − 40 m bmsl regional slowstand dated between ~ 11.5 and 10.6 cal kyr BP (Cooper et al. 2018; Engelbrecht et al. 2020). The height of this sea cliff is greater in the south and central regions of the study area relative to the observed height of this same sea cliff in north (Fig. 4c, e). The increased sea cliff height, which may reflect an increased depth of paleo-wave erosive action, effectively results in increased accommodation space and thus increased sediment accumulation on the seaward second wave-cut platform in the south/central regions of the study area. There is a notable change in the footwall elevation of the second wave-cut platform (north, 42–50 m bmsl; central, 50–57 m bmsl; south, poorly developed at around 50 m bmsl). The reason for this step change could not be discerned from the available data, and may relate to either difference in the resistance of the footwall rocks or perhaps to an antecedent structural control. The latter explanation has previously been illustrated at a study site near the Orange River mouth where electromagnetic data revealed a series of NNW-striking faults that strongly impact the nearshore geomorphology (Kirkpatrick and Green 2018).

A further difference between the marine geology of the northern region of the study site and its more southerly counterparts is observed in the elevation and morphology of the footwall architecture extending between the base of the second sea cliff and the break-in-slope of horizon 1 associated with the contact between unit 1 (Precambrian basement footwall) and unit 2. In the north (Fig. 4a, b), this segment of the seismic horizon 1 is relatively shallow, relatively devoid of a recent sediment veneer, and marked by a series of erosional troughs that are either related to the competency/resistance contrasts in the underlying basement lithologies, the depth of paleo sea-level stands during the stepped transgression since the last glacial maximum (e.g. Liu and Milliman 2004) or likely a combination of both factors. In contrast, the central transect reflects a deeper and more constantly dipping footwall architecture towards the contact between the two footwall lithologies (Fig. 4c, d). This trend is punctuated by only two minor (~ 2–3 m high) breaks or knickpoints; one at 72 m bmsl (corresponding to the last deglacial transgression dated by Runds et al. 2019) and one at 79 m bmsl. The southern transect appears to reflect a combination of the morphologies of the northern and central transects (Fig. 4e, f). That is, below the second sea cliff, the gradient dips moderately seaward and the basement is covered by ~ 2 m of recent sediment (as observed in the central transect) until a high-relief area devoid of sediment cover is encountered at ~ 60–73 m bmsl. This resistant feature can be traced to the shallow elevation basement rocks observed in the north of the study area (Fig. 5b). Throughout the study area, the contact between the Precambrian basement footwall and the Cretaceous clay footwall occurs at depths between 77 and 80 m bmsl in the south and central regions versus > 85 m bmsl in the north. Variability in the elevation of this regionally traceable contact has previously

been identified by Kirkpatrick et al. (2019a), who identified a range between 55 and 70 m bmsl.

The architectural features described in the preceding two paragraphs provide a basis for understanding the distribution of the recent sediment accumulations and their preservation. From our Sparker data, we were able to discern between two different sedimentary units (unit 3, significant gravel bodies; and unit 4, Cenozoic sediments (Table 1)). Delineation of further sub-units was unfortunately not possible due to the relatively low resolution of the Sparker data. We also did not conduct any dedicated geochronology and our temporal constraints are thus drawn from correlations with published data for the study sites described to the south of our study area (Table 1). Despite the occurrence of gravel beaches in these comparable study sites (notably in the Purple Target Area located 50 km south of Chameis Bay (Runds et al. 2019)), we were not able to confidently correlate the gravel bodies of unit 3 to any of the units described to the south. We were, however, able to tentatively correlate our unit 4 (unconsolidated Cenozoic sediments) to unit D of Runds et al. (2019), and unit 7 of Kirkpatrick et al. (2019a). Both of these previous workers have suggested an early to late Holocene age for these sediments. This is supported by the fact that our study site lies at depths ranging from 91 m bmsl which, according to the eustatic sea-level charts of Pether (2013a, b) and Clark et al. (2009), implies that the accumulated sediment must post-date the melt water pulse (MWP) 1a marine transgression (~ 14,000 years old; Cooper et al. 2018, and references therein).

These Holocene aged sediments show a variable distribution across the study site whereby the primary controls on its thickness distribution (Fig. 5) are a combination of the footwall architecture, the depth below the fair-weather wave base and possible antecedent structural controls that could not be discerned in this study (see Kirkpatrick and Green 2018). The thickest sediment packages are found at depths greater than 70 m bmsl, which roughly corresponds to the offshore regions underlain by the Cretaceous footwall lithology (Fig. 5). The accommodation space available for sediment accumulation and preservation can be considered on two different scales. The first is a highly localised scale in which individual architectural features impact the thickness distribution of the overlying sediment. For example, the depth (below mean sea level) of the knickpoint identified at the base of the first 10–20-m-high sea cliff plays a role in determining the amount of sediment that can be preserved on the associated seaward wave-cut platform (Fig. 4). The absolute breadth of this platform also has an obvious impact on available accommodation space (compare Fig. 4a–d to Fig. 4e, f). The second scale at which accommodation space can be considered is an average or regional (up to 8-km-long linear extent) scale which can be quantified using integration (Figs. 3 and 6). Between the footwall depth contours (isobaths) of 90 and 35 m bmsl, the average accommodation space in the study area shows a marked decrease towards the north of the seismic line 2–2′ (Fig. 6a). This average thus clearly measures the shallower shelf bathymetry of the northern region of the study area where the resistant Precambrian basement has not eroded as extensively or linearly as the seismic transects to the south. Importantly, when normalised to the linear extent of each transect, this integration measure correlates significantly with the thickness of sediment that has actually accumulated (within the defined depth interval) according to the equation $y = 3.12x + 53.06$ ($r^2 = 0.73$; Fig. 5c). The strength and consistency of this relationship, however, needs to be tested further using a greater number of data points, and across different depth intervals and at different study sites. Furthermore, when considering the relationships between the footwall architecture, accommodation space and sediment loading, factors such as sedimentation rate and wave- and tidal energy regimes also need to be taken into account.

Gravel characteristics and distributions as a proxy for diamond prospectivity

The Chameis Bay area represents the northern terminus of the linear beaches that predominate on the southernmost section of the Namibian Sperrgebiet coastline. Here, previous workers have shown that the raised gravel beaches locate on a narrow 300-m-wide tract of land situated on wave-cut platforms above the present-day sea level. Furthermore, of the six raised gravel beaches that represent the full series of these marine high-stand diamond deposits, the oldest and most elevated three beaches (the Late Pliocene–Early Pleistocene 'D', 'E' and 'F' beaches) are least well preserved (Jacob 2016; Kirkpatrick et al. 2019b). Within these beaches, the highest diamond grades are associated with gullies that have been incised into the Precambrian basement rocks in orientations controlled by the ambient jointing (60–70° and 120–140° (Jacob et al. 2006)).

Our study considers the gravel distributions in the offshore section (17–91 m bmsl) of Chameis Bay using two lines of geological data, viz. the distribution of unit 3 from seismic data, and gravel bodies and stringers intersected in the recovered borehole material. The seismic unit 3 was sporadically developed throughout the study area, although this sporadicity may partially be an artefact of the poor resolution of the Sparker data. Examples of where these gravel bodies were identified include erosional depressions in the Precambrian basement (e.g. Figure 3b), and to a lesser extent, in similar erosional depressions on the softer Cretaceous clay bedrock (e.g. Figure 3f). The latter occurrence appears reminiscent of the gravel barrier beach identified in the Purple Target Area by Runds et al. (2019); i.e. a mound-shaped feature occupying a basal position on the

low-gradient Cretaceous footwall, where the low gradient is hypothesised to facilitate beach preservation during rapid sea-level transgression. However, in our study area, these mound-like features were not traceable between adjacent seismic lines and thus probably do not represent preserved barrier beaches. An additional line of supporting evidence is the lack of distal, rounded cobbles in the basal gravels. These cobbles created the framework for the barrier beaches further south (Runds et al. 2019).

The gravels intersected during the drilling program are predominantly found overlying the Precambrian basement, and this is particularly true for the thickest gravel bodies intersected in the study area (Fig. 5a). Notable gravel intersections include localised erosional depressions in the broad shoreward wave-cut platform (shown by the rugged topography indicated by seismic horizon 1), the accommodation space provided by the second wave-cut platform (especially in the central region of the study area) and relatively high-gradient knickpoints associated with the high-relief feature in the south of the study area. The latter occurrence agrees well with previous work which has shown that a high bedrock gradient facilitates sediment reworking (or 'jigging') and typically leads to upgrading of the diamond grades along with their associated gravels (Kirkpatrick et al. 2019b). In the offshore region overlying the Cretaceous clay bedrock, the intersected gravels typically occur as multiple strata (or gravel stringers) each of which is relatively thin and poorly developed (Fig. 5a). Because the Cretaceous clay footwall is soft and easily erodible, the depressions that represent gravel (and diamond) trapsites were often likely transient in nature. We regard these as 'mobile' trapsites as further erosion to the soft footwall would result in remobilisation of the gravels, probably on a northward trajectory under the influences of long-shore drift. In comparison, the trapsites formed on the Precambrian basement will preferentially be in the form of the joint-controlled gullies (as observed on the onshore geology (Jacob et al. 2006)) and in erosive depressions formed by differential erosion of the variably competent lithologies of the Chameis Subterrane thrust sheet (i.e. Bogenfels Fm metasediments vs. Chameis Gate diamictites vs. mafic–ultramafic Bakers Bay Suite vs. Dernberg Fm metabasic rocks (Fig. 1b)). We deem these trapsites to be 'fixed' trapsites wherein the preservation potential for gravels and associated diamonds is much higher.

The recovered borehole material revealed that the gravels in the Chameis Bay area comprise a mixture of angular/sub-angular clasts that reflect the local (or proximal) geology and rounded/sub-rounded clasts that include exotic lithologies associated with rocks found on the Kaapvaal Craton (i.e. distal material). The relatively high proportion of proximal material relative to distal material is perhaps expected given that vast distance from the Orange River mouth (~ 115 km) and the known trend that coarse material outfall is highest close to the mouth (e.g. diamond carat size is known to decrease in a linear way with distance north of the mouth). Furthermore, the presence of a local non-perennial river draining into Chameis Bay represents a notable point source for the high proportion of proximal material. Some of this proximal material may, however, include clasts and diamonds from the raised Plio-Pleistocene-aged gravel beaches (e.g. Spaggiari et al. 2006; Jacob 2016) and from raised pocket beaches located 2 m above the present mean sea level (Apollus 1995). Erosion and reworking of this material into the nearshore 'fixed' trapsites will have been ongoing since the current sea-level stand reached its present level (~ 7.2 cal ka BP) and ultimately stabilised around ~ 5.5 cal ka BP (Compton 2001). A further, proximal source for this material is sediment that has been reworked from former shoreline deposits during sea-level rise associated with the Holocene transgression (Cooper et al. 2020).

Conclusion

The seismic stratigraphy and nearshore geomorphology of Chameis Bay was established using a combination of bathymetrical, seismic and sedimentary datasets. The stratigraphy offshore of Chameis Bay has been identified as being composed of four seismically defined sedimentary sequences (units 1–4). Analysis of these datasets to determine the architecture of the shelf for this region produced a low gradient shelf with the presence of two wave-cut platforms, separated by a sea cliff, where the wave-cut platforms have been infilled with a thin sequence of sediments of Cenozoic age. A regional break in slope can be traced throughout the region, as defined by the contact between the Precambrian footwall and the Cretaceous clay footwall, where a local increase in accommodation space occurs. Sediment accommodation space has been quantified using a novel integration measure which shows that the accommodation space, and thus sediment preservation potential, decreases from south to north within the study area. The decrease in accommodation space can be attributed to the Precambrian basement unit that has undergone lower degrees of erosion in the north. Both the Precambrian basement footwall and the Cretaceous clay footwall contain gullies that have the potential for the deposition of diamondiferous gravel bodies. As the Cretaceous clay unit acts as a 'mobile' trapsite and the Precambrian basement acts as a 'fixed' trapsite, the potential for the occurrence of a diamond-rich gravels is highest in the gullies on the latter footwall unit, especially in areas with a steep footwall gradient since this facilitates reworking and upgrade (Kirkpatrick et al. 2019b). Diamondiferous gravels are sourced from longshore drift of material emanating from the Orange River mouth, and from reworking of material contained in the various local raised beaches in the Chameis

Bay study area. The supply of abundant local angular clastic material, which is not diamondiferous, represents a dilution factor that must be accounted for when considering diamond potential within the study area.

Acknowledgements The authors would like to thank Namdeb Diamond Corporation (Pty) Limited, specifically C. August for enabling the project which represents the work conducted by the lead author (HF) for her B.Sc. Hons. thesis (Stellenbosch University, 2019). We gratefully acknowledge the assistance from, and fruitful discussions with J. Conradie, J. Jacob, M. Runds and L. Kirkpatrick. We further thank Professor J.A.G. Cooper, one other anonymous reviewer and editor Professor A.N. Green for their valuable comments which helped in strengthening the final submission. Financial support from DSI-NRF CIMERA (BvdH) is also acknowledged and duly appreciated.

References

Apollus L (1995) The distribution of diamonds on a Late Cainozoic gravel beach, southwestern Namibia. Dissertation, University of Glasgow

Beerbower JR (1964) Cyclothems and cyclic depositional mechanisms in alluvial plain sedimentation. Kansas State Geol Surv Bull 169(1):32–42

Bluck BJ, Ward JD, Cartwright J, Swart R (2007) The Orange River, southern Africa: an extreme example of a wave-dominated sediment dispersal system in the South Atlantic Ocean. J Geol Soc 164:341–351

Cecil CB (2003) The concept of autocyclic and allocyclic controls on sedimentation and stratigraphy, emphasizing the climate variable. In: Cecil CB, Edgar NT (eds) Climate controls on stratigraphy: SEPM Special Publication No. 77. Society for Sedimentary Geology, Tulsa, pp 13–20

Clark PU, Dyke AS, Shakun JD, Carlson AE, Clark J, Wohlfarth B, Mitrovica JX, Hostetler SW, McCabe AM (2009) The last glacial maximum. Science 325(5941):710–714

Compton J (2001) Holocene sea-level fluctuations inferred from the evolution of depositional environments of the southern Langebaan Lagoon salt marsh. South Africa the Holocene 11(4):395–405

Compton JS, Mulanisana J, McMillan IK (2002) Origin and age of phosphorite from the Last Glacial Maximum to Holocene transgressive succession off the Orange River, South Africa. Mar Geol 186:243–261

Cooper JAG, Green AN, Compton JS (2018) Sea-level change in southern Africa since the Last Glacial Maximum. Quatern Sci Rev 201:303–318

Cooper JAG, Masselink G, Coco G, Short AD, Castelle B, Rogers K, Anthony E, Green AN, Kelley JT, Pilkey OH, Jackson DWT (2020) Sandy beaches can survive sea-level rise. Nat Clim Chang 10(11):993–995

Davies JL (1964) A morphogenic approach to world shorelines. Zeitschrift Fur Geomorphologie 8:127–142

De Decker RH (1986) The geological settings of diamondiferous deposits on the inner shelf between the Orange River and Wreck Point. Thesis (unpublished), University of Cape Town, Namaqualand. M.Sc, p 258

De Wit M, Bhebhe Z, Davidson J, Haggerty SE, Hundt P, Jacob RJ, Lynn M, Marshall TR, Skinner C, Simithson K, Stiefenhofer J, Robert M, Revitt A, Spaggiari R, Ward JD (2016) Overview of diamond resources in Africa. Episodes 39(2):199–234

Dingle RV, Siesser WG, Newton AR (1983) Mesozoic and Tertiary geology of southern Africa. AA Balkema, Rotterdam

Engelbrecht L, Green AN, Cooper JAG, Hahn A, Zabel M, Mackay CF (2020) Construction and evolution of submerged deltaic bodies on the high energy SE African coastline: the interplay between relative sea level and antecedent controls. Mar Geol 424:106170

Frimmel HE (2018) The gariep belt. In: Siegesmund S, Basei MA, Oyhantçabal P, Oriolo S (eds) Geology of southwest gondwana. Springer, Cham, pp 353–386

Green AN (2009) Sediment dynamics on the narrow, canyon-incised and current-swept shelf of the northern KwaZulu-Natal continental shelf, South Africa. Geo-Mar Lett 29:201–219

Jacob J, Ward JD, Bluck BJ, Scholz RA, Frimmel HE (2006) Some observations on the diamondiferous bedrock gully trapsites on Late Cainozoic, marine-cut platforms of the Sperrgebiet, Namibia. Ore Geol Rev 28:493–506

Jacob J (2016) Contextualized risk mitigation based on geological proxies in alluvial diamond mining using geostatistical techniques. Dissertation, University of the Witwatersrand

Kalbskopf S (1987) Bedrock gullies, their patterns, morphology and relationship to major wave-cut shelves at CDM. CDM, (PTY) LTD. Internal report

Kirkpatrick LH, Green AN (2018) Antecedent geological control on nearshore morphological development: the wave dominated, high sediment supply shoreface of southern Namibia. Mar Geol 403:34–47

Kirkpatrick LH, Green AN, Pether J (2019a) The seismic stratigraphy of the inner shelf of southern Namibia: the development of an unusual nearshore shelf stratigraphy. Mar Geol 408:18–35

Kirkpatrick LH, Jacob J, Green AN (2019b) Beaches and bedrock: how geological framework controls coastal morphology and the relative grade of a Southern Namibian diamond placer deposit. Ore Geol Rev 107:853–862

Liu JP, Milliman JD (2004) Reconsidering melt-water pulses 1A and 1B: global impacts on rapid sea-level rise. Journal of Ocean University of China 3(2):183–190

Miller WR, Ramsay PJ, Leuci R, Bosman C (2000) Geophysical interpretation of the Kerbehuk Inshore Survey Block, Namibia. Council for Geoscience, South Africa (**Report No. 2000–0246, 23**)

Oelofsen A (2008) Late Cainozoic shallow marine diamond placers off the Northern Sperrgebiet, Namibia. M.Sc Thesis (unpublished), University of Cape Town, 193

Pether J (2013) The Last Transgression Sequence (LTS) and Formation of the Sediment Body, Namdeb Diamond Corporation (Pty) Ltd. Midwater Campaign Internal Report, 13

Pether J (2013) Chameis Geological Observations, Namdeb Midwater Campaign 2013, Namdeb Diamond Corporation (Pty) Ltd. Midwater Campaign Internal Report, 88

Rau G (2003) The integrated use of detailed geophysical, geological and oceanographic techniques to delineate and prioritize marine diamond placer deposits on the inner shelf, west coast, Central Namibia: EPL 1950 (Hottentot Bay) – a case study. Thesis (unpublished), Rhodes University, M.Sc, p 139

Ressler T (1998) WinXAS: A program for X ray absorption spectroscopy data analysis under MS-windows. J Synchrotron Radiat 5:118

Richardson K (2007) A perspective of marine mining within De Beers. The Journal of the Southern African Institute of Mining and Metallurgy 107:393–402

Robert C, Diester-Haass L, Paturel J (2005) Clay mineral assemblages, siliciclastic input and paleoproductivity at ODP Site 1085 off Southwest Africa: a Late Miocene-Early Pliocene history of Orange river discharges and Benguela current activity, and their relation to global sea level change. Mar Geol 216:221–238

Runds MJ, Bordy EM, Pether J (2019) Late Quaternary sedimentological history of a submerged gravel barrier beach complex, southern Namibia. Geo-Mar Lett 39:469–491

Spaggiari RI (2011) Sedimentology of Plio-Pleistocene gravel barrier deposits in the Palaeo-Orange River Mouth, Namibia: depositional history and diamond mineralisation. Dissertation, Rhodes University

Spaggiari RI, Bluck BJ, Ward JD (2006) Characteristics of diamondiferous Plio-Pleistocene littoral deposits within the paleo-Orange River mouth, Namibia. Ore Geol Rev 28:475–492

Stevenson IR, McMillan IK (2004) Incised valley fill stratigraphy of the Upper Cretaceous succession, proximal to the Orange Basin, Atlantic margin of southern Africa. J Geol Soc London 161:185–208

Stevenson IR (1999) The application of high resolution geophysical techniques for seismic stratigraphic analysis at an outcrop scale: a study from the Namaqualand Continental Shelf, west coast, South Africa. Dissertation, University of Reading

Williams R (1996) King of sea diamonds: the saga of Sam Collins. W.J Flesch and Partners (Pty) Ltd, Cape Town